Published in final edited form as:
Cell Signal. 2009 December ; 21(12): 1874–1884. doi:10.1016/j.cellsig.2009.08.003.

Lysophosphatidic Acid-induced Arterial Wall Remodeling: Requirement of PPAR γ but Not LPA_1 or LPA_2 GPCR

Yunhui Cheng[1,2], **Natalia Makarova**[1], **Ryoko Tsukahara**[1], **Huazhang Guo**[1], **Shuyu E**[1], **Patricia Farrar**[3], **Louisa Balazs**[4], **Chunxiang Zhang**[2,5], and **Gabor Tigyi**[1]

[1] Department of Physiology, University of Tennessee Health Science Center Memphis

[3] Department of Comparative Medicine, University of Tennessee Health Science Center Memphis

[4] Department of Pathology, University of Tennessee Health Science Center Memphis

[5] Department of Medicine, University of Tennessee Health Science Center Memphis

Abstract

Lysophosphatidic acid (LPA) and its ether analog alkyl-glycerophosphate (AGP) elicit arterial wall remodeling when applied intralumenally into the uninjured carotid artery. LPA is the ligand of eight GPCRs and the peroxisome proliferator-activated receptor γ (PPARγ). We pursued a gene knockout strategy to identify the LPA receptor subtypes necessary for the neointimal response in a non-injury model of carotid remodeling and also compared the effects of AGP and the PPARγ agonist rosiglitazone (ROSI) on balloon injury-elicited neointima development. In the balloon injury model AGP significantly increased neointima; however, rosiglitazone application attenuated it. AGP and ROSI were also applied intralumenally for 1 hour without injury into the carotid arteries of LPA_1, LPA_2, $LPA_{1\&2}$ double knockout, and Mx1Cre-inducible conditional PPARγ knockout mice targeted to vascular smooth muscle cells, macrophages, and endothelial cells. The neointima was quantified and also stained for CD31, CD68, CD11b, and α-smooth muscle actin markers. In LPA_1, LPA_2, $LPA_{1\&2}$ GPCR knockouts, Mx1Cre transgenic, $PPAR\gamma^{fl/-}$, and uninduced Mx1CreXPPAR$\gamma^{fl/-}$ mice AGP- and ROSI-elicited neointima was indistinguishable in its progression and cytological features from that of WT C57BL/6 mice. In $PPAR\gamma^{-/-}$ knockout mice, generated by activation of Mx1Cre-mediated recombination, AGP and ROSI failed to elicit neointima and vascular wall remodeling. Our findings point to a difference in the effects of AGP and ROSI between balloon the injury- and the non-injury chemically-induced neointima. The present data provide genetic evidence for the requirement of PPARγ in AGP- and ROSI-elicited neointimal thickening in the non-injury model and reveal that the overwhelming majority of the cells in the neointimal layer express α-smooth muscle actin.

Keywords

Balloon injury; lysophosphatidic acid; LPA_1; LPA_2; neointima; PPARγ

Address correspondence to: Gabor Tigyi, Department of Physiology, University of Tennessee Health Science Center, 894 Union Ave., Suite 426, Memphis, TN 38163, U.S.A. Telephone: (901) 448-4793, Fax: (901) 448-7126, gtigyi@physio1.utmem.edu.
[2]Present address: Department of Anesthesiology, New Jersey Medical School, University of Medicine & Dentistry of New Jersey, Newark, NJ 07101-1709

Disclosure/Duality of Interest
G.T. is founder and shareholder in RxBio Inc.

1. INTRODUCTION

Lysophosphatidic acid (LPA, 1-acyl-2-hydroxy-*sn*-glycero-3-phophate) and its ether-linked analog alkyl glycerophosphate (AGP, 1-alkyl-2-hydroxy-*sn*-glycero-3-phophate) are naturally occurring lipid mediators with growth factor-like effects in almost every mammalian cell type [1]. AGP and LPA elicit their biological responses through eight plasma membrane receptors that belong to the GPCR superfamily and intracellularly through the peroxisome proliferator-activated receptor γ (PPARγ) [2,3]. AGP and LPA are present in blood plasma [4] and become enriched after minimal oxidative modification of LDL [5,6]. The lipid rich core in human carotid endarterectomy specimens contains high concentrations of AGP and LPA [7] and upon plaque rupture could activate platelet aggregation and lead to atherothrombosis [5].

All major cell types of the arterial wall respond to LPA. In endothelial cells, LPA has been shown to regulate the expression of adhesion molecules, proliferation, apoptosis, permeability, motility and cell-to-cell contacts responsible for transendothelial permeability [8,9]. LPA induces vascular smooth muscle cell (VSMC) contraction, proliferation [10] and phenotypic transdifferentiation in vitro [6,11]. LPA and oxidized LDL inhibit macrophage/dendritic cell egress across endothelial cell monolayers [12,13]. LPA also stimulates the formation of platelet-monocyte aggregates, which are considered as an early marker of acute myocardial infarction [14,15].

Yoshida and colleagues were the first to test lumenally applied LPA on the non-injured arterial wall *in vivo*[16]. These authors infused LPA through the external carotid artery of rats into a ligated section of the common/internal carotid artery that was rinsed free of blood and maintained close to the mean arterial perfusion pressure. In this model, which involves no mechanical injury or the removal of endothelial cells in the common carotid artery, after 1-hour exposure to unsatured but not to saturated species of low micromolar LPA leads to neointima development. These authors interpreted their observation as if a yet unknown LPA GPCR activated only by unsaturated species of LPA. However, the structure-activity relationship of neointima induction does not match that of the known LPA GPCRs but matches the structure-activity relationship of PPARγ activation by LPA.

LPA is an agonist of the nuclear transcription factor PPARγ [2]. PPARγ has long been implicated in atherogenesis [17,18]. Many compounds activate PPAR, including the synthetic drug Rosiglitazone (ROSI) of the thiazolidinedione family, oxidized phospholipids, fatty acids, eicosanoids, and oxidized LDL. PPARγ is expressed in macrophages/monocytes, vascular smooth muscle cells, endothelial cells, and is highly expressed in atherosclerotic lesions and hypertensive vascular wall [17]. GW9662, a specific irreversible antagonist of PPARγ [19] completely abolished AGP, LPA and ROSI-induced neointima formation in the rat model [6]. Although, these lines of evidence support the role of PPARγ as the receptor responsible for the neointimal thickening elicited by AGP and LPA, the pharmacological evidence does not exclude the possibility that LPA GPCR mediate this response alone or through the indirect activation of PPARγ. Several investigators reported that systemic and chronic administration of ROSI attenuates neointima in models with mechanical injury of the arterial wall which is different from findings reported using the non-injury model [20,21].

Here we compared the effects of AGP and ROSI on arterial wall remodeling in a balloon injury model with that in the non-injury model and found that these agents elicit model-dependent different responses. We pursued a gene knockout (KO)-based strategy to seek the identification of the LPA receptor subtype(s) necessary for the neointimal response in the non-injury model. We tested AGP and ROSI in LPA_1, LPA_2, LPA_1 and LPA_2 double knockout (DKO), and in inducible conditional PPARγ knockout mice targeted to VSMCs, macrophages and endothelial

cells by the Mx1Cre promoter. We also sought to characterize the phenotypic properties of cells involved in LPA-elicited neointimal thickening and found that the overwhelming majority of the cells in the neointimal layer express α-SMA characteristic of the VSMC lineage. Our findings showed that $LPA_{1\&2}$ GPCR KO mice behave like wild type (WT) mice whereas, PPARγ KO fail to develop AGP- and ROSI-induced neointimal thickening.

2. METHODS

2.1. Reagents

1-O-octadecenyl glycerophosphate (AGP 18:1) was purchased from Avanti Polar Lipids (Alabaster, AL). Rosiglitazone (ROSI) was from ALEXIS Biochemicals, Inc. (Plymouth Meeting, PA). TRIzol Reagent, DNase I, and the ThermoScript RT-PCR System for First-Strand cDNA Synthesis were from Invitrogen (Carlsbad, CA). The RT2 Real-Time SYBR Green/ROX kit was purchased from SuperArray (Frederick, MD).

2.2. Quantitative RT-PCR

Total RNA was prepared using TRIzol reagent from mouse common carotid artery from which the adventitia had been peeled off. One μg of total RNA was digested with DNase I and used for the subsequent synthesis of cDNA using the First Strand Synthesis kit as recommended by the manufacturer. The following primer pairs were used: LPA_1, (forward) GTCTTCTGGGCCATTTTCAA and (reverse) TCATAGTCCTCTGGCGAACA; LPA_2, (forward) GGGCCAGTGCTACTACAACG and (reverse) ACCAGCAGATTGGTCAGCA; LPA_3, (forward) GAATTGCCTCTGCAACATCTC and (reverse) ATGAAGAAGGCCAGGAGGTT; LPA_4, (forward) TCTGGATCCTAGTCCTCAGTGG and (reverse) CCAGACACGTTTGGAGAAGC; LPA_5, (forward) CGCCATCTTCCAGATGAAC and (reverse) TAGCGGTCCACGTTGATG; and GAPDH, (forward) CTGCACCACCAACTGCTTAG and (reverse) GGGCCATCCACAGTCTTCT. The primer sets were designed with a melting temperature of 59–61°C. Amplicon size was 50–200 bases. Amplification was performed for 40 cycles at 94°C/15 sec and 60°C/60 sec. Quantitative values were obtained from the threshold cycle value (Ct) as previously described. [22]

2.3. Immunofluorescence staining

Cryosections dipped in 4% buffered paraformaldehyde were blocked in 10% goat serum and incubated with rat anti-mouse CD31 (anti-PECAM-1 rat monoclonal antibody, 1:400 dilution; RDI Inc.; Concord, MA), or anti-mouse CD11b (anti-Mac-1 rat monoclonal antibody, 1:100 dilution; BD Pharmingen; San Diego, CA), or anti-mouse CD68 (anti-macrosialin rat monoclonal antibody, 1:400 dilution; ABD SeroTec; Oxford, UK) antibodies. Anti-rat fluorescein-conjugated secondary antibody was used at a 1:200 dilution (Vector Laboratories; Burlingame, CA). Cell nuclei were stained with DAPI. The MOM kit (Vector Laboratories) was used for α-smooth muscle actin (α-SMA) staining. Briefly, after fixation and permeabilization, tissue sections were incubated with mouse IgG blocking reagent for 1 h, followed by 1:200 diluted anti-α-SMA antibody (1:400 dilution; DAKO; Carpinteria, CA) and then 1:200 diluted Texas Red conjugated anti-mouse antibody (1:200 dilution; Vector Laboratories). For the double staining of mouse carotid artery sections, α-SMA staining was carried out using the MOM kit on anti-CD11b- or anti-CD68-stained sections. The fluorescence was observed by Nikon Eclipse 80i fluorescence microscope. Merged images for double-stained sections were generated by the NIS-Elements (V2.1, Nikon Instruments) image analysis software.

2.4. Rat carotid artery balloon injury model

The animal procedures were approved by the Institutional Animal Care and Use Committee at the University of Tennessee and were consistent with the Guide for the Care and Use of Laboratory Animals (National Institutes of Health publication 85-23, revised 1985). Carotid artery balloon injury was induced in male Sprague-Dawley rats (230 to 300 g) anesthetized with ketamine (80 mg/kg) and xylazine (5 mg/kg). Under a dissecting microscope, the right common carotid artery was exposed through a midline cervical incision. A 2F Fogarty catheter (Baxter-Edwards) was introduced via an arteriotomy via the external carotid artery, and then the catheter was advanced to the proximal edge of the omohyoid muscle. The balloon was inflated with saline and withdrawn three times from under the proximal edge of the omohyoid muscle to the carotid bifurcation. The common and internal carotid arteries were clamped and a 100 μl aliquot of AGP (10 μM), ROSI (10 μM), or vehicle was instilled into the injured segment via a PE-10 catheter and was incubated for 60 min. Subsequently, the catheter was withdrawn and the external carotid artery was ligated with 6-0 silk suture. The clips at the common and internal carotid arteries were released, and blood flow in the common carotid artery was restored. Three weeks after injury the carotids were dissected and processed for histology as described for the mouse specimens above. Each group consisted of six rats.

2.5. Transgenic and Knockout Animals

LPA_1 and LPA_2 knockout breeders on C57BL/6 background were generously provided by Jerold Chun (Scripps Institute, CA) and have been characterized previously [23–25]. $LPA_{1\&2}$ double knockout (DKO) mice were obtained by crossing homozygous LPA_1 males with LPA_2 females. Genotyping of the DKO mice was done as described by Contos et al. coworkers [24]. The C57BL/6-Mx1Cre mouse line was made available by Dr. Matthew Breyer (Vanderbilt University) that allows the differential, interferon (IFN)-inducible targeting of the Cre recombinase to vascular and renal endothelium, vascular smooth muscle cells and macrophages [26,27]. The Mx1Cre is induced intraperitoneal injection of the IFN-inducer synthetic double-stranded RNA polyinosinic-polycitidylic acid (pIpC, Sigma-Aldrich, St. Louis, MO). Dr. Mark Magnuson (Vanderbilt University) generously provided us a mouse line with exon 2 of PPARγ has been flanked by LoxP sites on the C57BL/6 background [28]. $PPAR\gamma^{fl/-}$ mice were bred with homozygous *Mx1Cre* mice to generate mice that are $PPAR\gamma^{fl/-}$XMx1Cre. Upon Mx1 induction with pIpC in $PPAR\gamma^{fl/-}$XMx1Cre mice, Cre recombines the single PPARγ allele creating a conditional knockout [28–30]. These induced conditional KO mice will be referred to as ΔPPARγ. Thus, ΔPPARγ mice allowed the targeted disruption of PPARγ in the three most important cell types – vascular endothelium, VSMC and macrophages [27,29] – involved in vascular remodeling whereas, littermates not induced with pIpC injections served as controls. In addition, Mx1Cre transgenic mice and pIpC-induced $PPAR\gamma^{fl/-}$ mice were also used to examine AGP- and ROSI-induced vascular wall remodeling.

2.6. Monitoring PPARγ recombination

Genotyping of Mx1/CreXPPAR$\gamma^{fl/-}$ and PPAR$\gamma^{fl/-}$ mice was done as described by Jones et al.[28] The position of the genotyping primers and their respective PCR products is shown in Supplemental Fig. 1A & B. Examples of the wild-type (WT) Mx1/CreXPPAR$\gamma^{fl/-}$ genotype (mouse #23) and PPAR$\gamma^{fl/-}$ genotype (mouse #24) are shown in Supplemental Fig. 1C. The following genotyping primers were used: A_1, (forward) 5′-TACTTAATGTCATGATGATCTGT-3′; A_2, (reverse) 5′-GATAAGACAG CACAACAATGTTC-3′; B_1, (reverse) 5′-GCTCCTGAGTGCTAATATTAAAG-3′; and B_2, (forward) 5′-CCATGGACTAATGCTGTAATATTA-3′ Cre-specific primers – (forward) 5′-ACCTGAAGATGTTCGCGATTATCT-3′ and (reverse) 5′-ACCGTCAGTACGTGAGATATCTT-3′ – were used, yielding a 370-bp fragment (Supplemental Fig. 1D). Amplification was done using a 200-ng template for 40 cycles (Tag

DNA Polymerase; New England Biolabs; Ipswich, MA). Two weeks after pIpC induction of young animals RT-PCR for PPARγ mRNA expression was done using peritoneal macrophages, carotid arteries, or abdominal aorta samples (Supplemental Fig. 1D). For PPARγ the 5′-GGAAAGACAACAGACAAATCACC-3′ (forward) and 5′-ATTCAGCTTGAGCTGCAGTTC-3′ (reverse) primers were used the amplicon yielding a 558 bp fragment. For quantitative monitoring of pIpC-induced Mx1Cre-mediated recombination of PPARγ, 18 mice were randomly divided into two equal groups. One group was injected i.p. with 250 μl of pIpC (2 mg/ml) on days 1, 3, 5, and 7; the others received vehicle. Two weeks after the last injection, the mice were anesthetized with ketamine and xylazine and injected i.p. with 5 μl of sterile PBS. About 5×10^5–10^6 macrophages per mouse were collected from the peritoneal wash by centrifugation and the common carotid artery and the aorta were dissected. RNA purified using TRIzol was pooled from three mice, yielding three samples (treated separately) from the nine mice. One μg of RNA was digested with DNase I and used for the subsequent synthesis of cDNA, using the First Strand Synthesis kit. The following primer pairs were used: PPARγ, (forward) 5′-CATGCTTGTGAAGGATGCAA-3′ and (reverse) 5′-CCCAAACCTGATGGCATT-3′; and GAPDH, (forward) 5′-CTGCACCACCAACT GCTTAG-3′ and (reverse) 5′-GGGCCATCCACAGTCTTCT-3′. Amplification was performed for 40 cycles at 94°C/15 sec and 60°C/60 sec. Quantitative values were obtained from the Ct. ΔCt was defined by subtracting the average Ct value of PPARγ from the corresponding Ct value of the GAPDH gene in a given sample. Results were expressed as fold difference (N) in gene expression relative to GAPDH, where $N = 2^{(\Delta Ct\ pIpC\ -\ \Delta Ct\ vehicle)}$. In peritoneal macrophages, the PPARγ transcript number decreased by 95% after pIpC induction, whereas in the carotid tissue the decrease was 87% (Supplemental Fig. 1E).

2.7. Mouse model of neointima induction

The surgical procedure for exposing and cannulating the external carotid artery originally developed by Yoshida et al. [16] rats was adopted to mice. Briefly, the right carotid arteries of anesthetized adult (8–12 week) and sex-matched mice (20–30 g) was surgically exposed. The caudal origin of the common carotid artery was ligated using a vessel clip, followed by exposure and ligation of the internal carotid artery above the bifurcation. The external carotid artery was then exposed and a polyethylene catheter was inserted into the external carotid such that it never reached the common carotid artery, thereby avoiding mechanical injury to this segment of the vessel. The clip occluding the common carotid artery was temporarily released, and the vessel was rinsed with a retrograde injection of 100μl physiological saline to remove residual blood. The vessel was again clipped, and 50 μl of treatment solution containing 5μM AGP or ROSI dissolved in 3% DMSO PBS (vehicle) was injected under pressure. After 60 min of incubation, the cannula was withdrawn, the external carotid artery was ligated, and blood flow was restored by removing the clips. Three weeks post surgery the animals were euthanized, and the common carotid artery from the jugular arch to the bifurcation was dissected on both sides, snap frozen in liquid N_2-cooled isopentane and processed for histological analysis. Cryostat sections (~5 μm) were cut and stained with hematoxylin and eosin, Masson's trichrome stain (Richard-Allan Scientific Inc.) or processed for immunohistological staining. Intima-to-media ratios were measured using the NIH Image (version 1.62) software. Groups consisted of four-to-ten animals per treatment or control group. Intima-to-media ratios (mean ± SEM) were compared between the appropriate groups using Student's t-test and $p < 0.05$ was considered statistically significant.

3. RESULTS

3.1. Differential effects of AGP and ROSI on injury-induced neointima

Several literature reports describe the inhibitory effect of the PPARγ agonist ROSI on injury-induced neointima [20,21]. In contrast, in the non-injury model using topical application of

ROSI or LPA we and others [6,16] have found that these PPARγ agonists elicited arterial wall remodeling that includes neointimal growth. To resolve this apparent contradiction, we hypothesized that the mechanisms causing neointima differ between the injury and the non-injury models. Consequently, these agents might exert different effects in these two models. To examine this possibility, we applied a balloon injury model of the rat carotid followed by ROSI or AGP treatments. The injury-induced neointima increased significantly by AGP application following injury ($p < 0.02$, Figure 1). However, in agreement with previous reports, ROSI application following balloon injury attenuated neointima formation; although, this attenuation was not statistically significant ($p=0.24$). These observations suggest different mechanisms for AGP and ROSI in this balloon injury model and warn against a direct comparison between this and the non-injury model.

3.2. Expression of LPA GPCR subtypes in the mouse carotid

QPCR was used to assess the expression of $LPA_{1–5}$ GPCR. Transcripts were detected with a rank order of $LPA_1 > LPA_4 \gg LPA_2 = LPA_3 > LPA_5$ (Fig 2A) in both the carotid and aortic tissue (not shown). LPA_1, LPA_2, LPA_3, and LPA_4 GPCR are 12-, 30-, 100-, and 1.5-times less sensitive to AGP than LPA [31,32], respectively. In contrast, AGP is more potent than LPA inducing arterial wall remodeling [6]. LPA_4 KO mice only became available after the conclusion of the experiments presented herein and were not included in the present study. Although LPA_3 was reported to prefer unsaturated LPA species over saturated ones [33], this is not unique to LPA_3 but also found at LPA_1 and LPA_2 [31]. Due to the 100-fold lesser potency of AGP over LPA at the LPA_3 GPCR combined with the low abundance of its transcripts in the carotid LPA_3 KOs were not included in the study. The ligand selectivity of the LPA GPCR tend to discount but do not exclude the role of these receptors in AGP-induced arterial wall remodeling.

3.3. Lumenally applied AGP and ROSI elicit vascular remodeling in the uninjured mouse carotid artery

In an effort to examine the contribution of the different cell surface and intracellular LPA receptors to AGP-elicited vascular remodeling we adopted the carotid infusion model to mice. Similarly to our findings in rats [6], infusion of vehicle to the mouse carotid failed to induce remodeling (Fig. 2B and Fig. 3A). In contrast, a brief 60 min application of 2.5 μM AGP elicited multilayered neointima (Fig. 2C). The PPARγ agonist ROSI (2.5 μM) also elicited arterial wall remodeling (Fig. 2E). No apparent morphologically distinguishable features were found between intimal thickening elicited by AGP or ROSI. Neointima development was accompanied by changes in the media as indicated by the blue staining in the trichrome-stained slides (Fig. 2D & E) in segments of the common carotid artery not subjected to mechanical injury either by cannulation or clipping. The arteries taken from the contralateral side showed no visible alteration upon microscopic observation (data not shown). The beginning of intimal thickening was clearly observed by the second week and progressed up to the fourth week, the latest time point examined. The neointimal layer developed in response to AGP was not stained with anti-CD31 (Fig. 3C) but strongly reacted with anti-α-SMA antibody (Fig. 3D). Using double staining, only a few cells in the neointima expressed the CD68 marker (Fig. 3E) and CD11b positive cells were scarce (Fig. D). Similar immunocytological findings were noted in the ROSI treated mice (Figure 4A–F).

3.4. Neointimal responses in LPA GPCR KO mice

LPA_1, LPA_2, and DKO mice were subjected to intracarotid application of 2.5 μM AGP or ROSI and the carotids were isolated 3 weeks later and neointima formation was quantified. Intima-to-media ratio measurements in LPA_1, LPA_2, and DKO mice showed that AGP (Fig. 5A, Fig. 6A) and ROSI (Fig. 5B) elicited neointima development that was indistinguishable

from that seen in WT mice. The cells comprising the neointima were not stained with anti-CD31 (Fig. 6B) but showed strong immunoreactivity with the anti-α-SMA antibody (Fig. 6C). The neointima contained scattered CD68 positive cells (Fig. 6D), whereas CD11b positive cells were scarce (Fig. 6E). Double staining with anti-SMA and CD68 (not shown) or CD11b (Fig. 6F) antibodies showed distinct populations of cells expressing the two markers that was similar to the staining patterns seen in WT animals (Fig 3E & F and Fig. 4D–F). The immunohistological staining of the single KO mice showed features (not shown) that were similar to those seen in DKO or WT mice. These observations did not support the requirement for LPA_1 and LPA_2 GPCR in AGP- and ROSI-elicited arterial wall remodeling; thus we focused our investigation to PPARγ.

3.5. Neointimal responses in conditional PPARγ KO mice

Knocking out PPARγ causes embryonic lethality, hence we were limited to the availability of conditional KOs that reach adulthood. We chose the Mx1CreXPPARγ$^{fl/-}$ mouse because in this strain we could experimentally activate Cre-mediated recombination through the Mx1 promoter in the endothelium, VSMC, and macrophages [26,27]. The added benefit of inducible Cre-mediated recombination was that we could compare induced and uninduced littermates. In addition, we examined mice from the parental strains Mx1Cre and PPARγ$^{fl/-}$ for their responses to intracarotid application of AGP and ROSI. In these experiments Mx1Cre mice showed neointima similar to WT mice (Figs. 7A and 8A & B). PPARγ$^{fl/-}$ littermate mice were randomly assigned to two groups, one of which received vehicle, the other was induced with pIpC three weeks prior to carotid surgeries. The uninduced (vehicle injected) group was included to determine whether deletion of one PPARγ allele has any effect on arterial wall remodeling elicited by the two compounds. The pIpC induced control group was designed to assess the effect of pIpC pretreatment on AGP- and ROSI-elicited arterial wall remodeling. Three weeks after these pretreatments the animals were exposed to either vehicle, 2.5 μM AGP, or ROSI for 1 h. After 21 days post carotid surgery the arteries were processed for histology and immunohistology to examine the arterial wall. Determination of the intima-to-media ratio regardless of pretreatment by vehicle or pIpC in the AGP-treated animals showed increases that were identical to those seen in WT animals (Figs. 7B & G). Similarly, when ROSI was infused into the carotids of pretreated animals the intima-to-media ratio increased (Fig. 7H, Fig. 8C & D). These results indicate that neither presence of only a single PPARγ allele nor pretreatment with pIpC abolished arterial remodeling elicited by AGP or ROSI.

Littermates of Mx1CreXPPARγ$^{fl/-}$ animals were randomly assigned to two pretreatment groups to receive either pIpC induction or vehicle. After a 3-week period the carotids of these animals were exposed to either 2.5 μM AGP, 2.5 μM ROSI, or vehicle. Carotid arteries of vehicle pretreated Mx1CrexPPARγ$^{fl/-}$ animals three weeks after AGP or ROSI treatment showed significant increases in intima-to-media ratio (Figs. 7C, G, H, Figs. 8E & F). The neointima-to-media ratios were similar to that seen in WT animals or PPARγ$^{fl/-}$ animals, establishing that the Mx1CreXPPARγ$^{fl/-}$ genetic background without pIpC induced Mx1Cre recombination develops arterial wall remodeling in response to AGP or ROSI. In sharp contrast, in the pIpC-induced ΔPPARγ animals AGP or ROSI treatment failed to alter the intima-to-media ratio (Figs. 7D, G, H, F, Figs. 8G & H). These results indicate that conditional KO of PPARγ completely abolishes the arterial wall remodeling elicited by AGP or ROSI. Carotid arteries obtained from every group of animals were also stained with anti-CD31, anti-α-SMA, anti-CD68, and anti-CD11b antibodies. In those groups of animals that showed increased intima-to-media ratios the immunohistological profile was qualitatively indistinguishable form that of the WT treated with AGP or ROSI. In ΔPPARγ animals that showed no alterations in the intima-to-media ratio we did not observed an increase in SMA positive cells (Fig. 7F, and Fig. 8H) or alterations in the CD68 or CD11b (not shown) marker-bearing cell populations.

4. Discussion

Arterial wall remodeling is considered a prelude to atherosclerotic disease and its pharmacological modulation is of significance in the prevention of several associated pathologies. Injury-induced and post-angioplasty arterial wall remodeling also represent human pathologies that would benefit from pharmacological intervention. The growth factor-like phospholipid mediator LPA has been shown to induce arterial wall remodeling in the absence of injury following only a brief 1-h-long topical application into the lumen of the carotid artery [6,16]. In the present study we sought genetic evidence for the role of LPA_1 and LPA_2 GPCRs and the intracellular LPA receptor PPARγ in this chemically-induced model of arterial wall remodeling.

First, we attempted to resolve the apparent contradiction between chronic ROSI-induced attenuation of injury-elicited neointima [20,21] and the ROSI-induced neointimal response in the non-injury model by comparing AGP and ROSI effects in the two models. We hypothesized that the mechanisms underlying neointima formation in the chemically-induced and injury-induced models differ leading to the opposite outcome in the response to ROSI application. In the balloon injury model AGP significantly augmented the intima-to-media ratio over that elicited by the injury (Fig. 1A–C). In contrast, ROSI treatment did not cause either a significant attenuation or augmentation in the intima-to-media ratio relative to the injury control, although the neointima in this treatment group was lesser than in the injury control group (Fig 1A & D). This set of experiments clearly indicates that ROSI and AGP application to an injured vessel with disrupted epithelium elicit different outcomes. Future experiments will be conducted using the KO mouse models to evaluate the role of LPA GPCR and PPARγ after vessel wall injury.

Our second objective was to establish and validate a chemically-induced arterial remodeling model in the mouse. We scaled down the treatment from the previously reported rat model [6,16] and found that in C57BL/6 mice, which represents the genetic background of our knockouts, lumenal application of AGP elicited carotid remodeling at low micromolar concentrations (Fig. 2C & D). No such changes were found in vehicle treated (Fig. 2B) or sham operated animals or in the contralateral carotid of AGP-treated mice. Just as in the rat, in mice luminal intracarotid application of ROSI (Fig. 2E & F) mimicked the effects of AGP when applied at the same concentration and over the same time course. This observation extended the utility of this model from the rat to the mouse, creating the opportunity for inclusion of transgenic and knockout mice in our experiments.

The cellular markers of the treated carotids were examined using antibodies specific to Von Willebrand factor (CD31), α-SMA, the pan macrophage marker CD68, and the CD11b marker, which is expressed by tissue macrophages including dendritic cells. Carotid arteries collected from AGP- or ROSI-treated WT mice showed a single layer of CD31 positive cell layer (Fig. 3C, Fig. 4B) indicating that the cells in the neointima lacks this endothelial cell marker. The neointimal layer showed very strong staining with the α-SMA marker (Fig. 3D, Fig. 4C) suggesting that the AGP- or ROSI-induced neointima involves the expansion of a cell lineage expressing this smooth muscle cells and myofibroblast marker. Infiltration by cells of the macrophage lineage has been noted in atherosclerotic lesions as well as in the injury-induced neointima [34–36]. We applied double immunostaining for α-SMA cells and CD68 markers in search for double positive cells but failed to detect double positive cells (Fig. 3E). Immunostaining for the CD11b marker showed few cells localized to the media-adventitia boundary. We did not detect double CD11b and α-SMA immunoreactive cells (Fig. 3F,Fig. 4F). These observations provide important insight into the mechanism of AGP-induced arterial wall remodeling. Llodra et al.[13] reported that LPA blocks the egress of macrophage/dendritic cells from the subendothelium leading to their accumulation. Our experiments showed few

CD68 and CD11b positive monocytoid cells within multiple layers of α-SMA positive cells. Thus in this model the overwhelming majority of neointimal cells expresses α-SMA marker which tends to favor a hypothesis that the vascular smooth muscle lineage dominates the cell type responsive to AGP or ROSI stimulation. Whether macrophages are retained initially and cytokines derived from them lead to a secondary immigration and/or proliferation of α-SMA positive cells remains to be subject in future studies. Even if this hypothesis will turn out to be correct, the initiating signal that attracts macrophages into the subendothelium would have to originate from the AGP-activation of cells resident to the normal carotid wall. LPA through the LPA_1 and LPA2 GPCRs has been shown to induce the expression of proinflammatory chemokines including MIP-1beta, IL-8, and MCP-1[9,37,38]. Thus if LPA_1 and/or LPA_2 receptors were required for the accumulation of macrophages leading to neointima, we should have found no macrophage accumulation and neointima in the DKO mice but this was not supported by the experimental findings. Because in rats we found that the effects of LPA or AGP on carotid artery remodeling were indistinguishable from that of ROSI, we tested this compound also. The cellular composition of the ROSI-elicited neointima resembled those in AGP treated carotids (Fig. 4). These similarities provide added circumstantial support to the hypothesis that these compounds activate a similar mechanism leading to arterial wall remodeling.

LPA_1, LPA_2, and DKO mice have been generated and show no spontaneous vascular pathology [24]. Because LPA_1 and LPA_2 both are activated by AGP [31,32], we focused initially on their role in LPA-induced arterial wall remodeling. Because of the availability of these single KOs, we also crossed them and established DKO animals. Both AGP and ROSI elicited neointima in the three KO strains that were statistically and immunohistologically indistinguishable from that seen in the WT mice (Figs. 5 & 6). LPA GPCR are activated by both saturated and unsaturated acyl-LPA with a rank order of potency of acyl-LPA > alkyl-GP [31]. Only LPA_5 prefers AGP over LPA [32] but transcripts of this receptor subtype were the least abundant in the mouse carotid (Fig. 2A). Moreover, LPA GPCRs do not show stereoselectivity to AGP [39]. The structure-activity relationship for LPA-induced neointima formation is markedly different from that described for LPA GPCR[6]: 1) it shows a rank order of alkyl-GP > acyl-LPA, 2) only unsaturated but not saturated fatty acyl species stimulate lesion formation, and 3) the effect shows stereoselectivity for 1-O-AGP over 3-O-AGP. Whereas, LPA-induced cell VSMC proliferation and migration is blocked by pertussis toxin [10], pretreatment by this toxin only slightly attenuated, but did not abolish neointima formation [6]. Diacylglycerol pyrophosphate, a competitive antagonist of the LPA_3 and LPA_1 receptors [40], produced only a partial inhibition of neointima formation. Based on the present results from the LPA GPCR KOs we now expand our previous indirect pharmacological observations and conclude that neither LPA_1 nor LPA_2 receptors are required for AGP- and ROSI-induced arterial wall remodeling.

Because the specific PPARγ antagonist GW9662 fully abolished arterial wall remodeling in rat carotids exposed to AGP, or ROSI, we examined the effect of these agents in conditional PPARγ KO mice. Knocking out PPARγ leads to embryonic lethality and the inducible conditional KO of PPARγ activated by the IFN-regulated Mx1Cre transgene offers an ideal model system in our case because the Mx1Cre is predominantly expressed in endothelial cells, vascular smooth muscle cells and in also in macrophages [26,27], which represent the three cell types implicated in the literature in neointima formation. The inducible Mx1Cre-regulated recombination of the single floxed PPARγ allele also provided littermate controls that were not exposed to pIpC induction. We also evaluated the effect of pIpC induction in $PPAR\gamma^{fl/-}$ animals three weeks prior to AGP or ROSI treatment of the carotid artery to determine whether it would alter the responsiveness of the arterial wall. Quantitative RT-PCR for PPARγ showed that three weeks was sufficient to induce the recombination of the floxed PPARγ allele with high penetration although recombination was not complete (Supplemental Fig. 1). Topical

intracarotid application of AGP or ROSI in pIpC-induced PPARγ$^{fl/-}$ animals elicited arterial wall remodeling with intima-to-media ratio indistinguishable from that seen in WT animals (Fig. 7G & H). These findings indicate that pIpC induction does not affect the arterial wall remodeling elicited by AGP and ROSI. Furthermore, these results also establish that deletion of one PPARγ allele does not attenuate AGP- or ROSI-induced neontima. Uninduced Mx1CreXPPARγ$^{fl/-}$ developed neointima in response to the treatments indicating that spontaneous recombination and the ensuing deletion of this nuclear hormone receptor, if present, is not sufficient to abolish arterial wall remodeling. The immunohistological observations of the arterial wall of these AGP or ROSI treated mice showed qualitative features that resembled those seen in WT animals (Fig. 7 & 8). In sharp contrast, in ΔPPARγ mice AGP or ROSI failed to cause a significant change in intima-to-media ratio (Figs. 7G & H). Immunohistological examination of carotid arteries taken from these mice showed no α-SMA positive cells between the endothelium and the internal elastic lamina (Figs. 7F and Fig. 8H). These observations taken together provide genetic evidence for the requirement of PPARγ in the arterial remodeling elicited by AGP and ROSI. The present findings combined with our previous report showing that the PPARγ antagonist GW9662 fully blocked AGP- and ROSI-induced arterial wall remodeling in rats, now provide two independent lines of evidence for the requirement of PPARγ in neointima development in the non-injury model.

LPA and AGP activate platelets, stimulate the formation of platelet-monocyte aggregates [15], and accumulate in the lipid rich core of human atherosclerotic plaques. LPA production in blood is linked to platelet activation [41]. LPA activates the expression of V-CAM and E-selectin adhesion molecules in endothelial cells which promote cell adherence and invasion of the vessel wall by blood cells [8]. LPA also stimulates proinflammatory cytokine production [37,42] and inhibits the egress of macrophages from the subendothelium [13]. This abundance of evidence combined with our present observations support the role of LPA in vascular wall remodeling and the present study underlines the importance of PPARγ as an important molecular target in this pathology.

Supplementary Material

Refer to Web version on PubMed Central for supplementary material.

Acknowledgments

We thank Ms. Jian Yang for expert assistance with the histology, Ms. Lillian Zalduondo and Ms. Melinda McCarty for animal care.

Sources of funding: This study was supported by NIH grant HL79004 (GT), a Thomas Gerwin Graduate Student Fellowship (SE), and American Heart Association grant 0530106N (CZ).

Abbreviations

AGP
1-alkyl-2-hydroxy-*sn*-glycero-3-phophate

α-SMA
α-smooth muscle actin

ΔPPARγ
pIpC-induced conditional knockout PPARγ$^{fl/-}$XMx1Cre mouse

DKO
LPA_1 and LPA_2 double knockout mouse

EEL
external elastic lamina

IEL
internal elastic lamina

LDL
low density lipoprotein

pIpC
polyinosinic-polycitidylic acid

PPARγ
peroxisome proliferator-activated receptor γ

ROSI
Rosiglitazone

VSMC
vascular smooth muscle cell

References

1. Siess W, Tigyi G. J Cell Biochem 2004;92(6):1086–1094. [PubMed: 15258894]
2. McIntyre TM, Pontsler AV, Silva AR, St Hilaire A, Xu Y, Hinshaw JC, Zimmerman GA, Hama K, Aoki J, Arai H, Prestwich GD. Proc Natl Acad Sci U S A 2003;100(1):131–136. [PubMed: 12502787]
3. Tsukahara T, Tsukahara R, Yasuda S, Makarova N, Valentine WJ, Allison P, Yuan H, Baker DL, Li Z, Bittman R, Parrill A, Tigyi G. J Biol Chem 2006;281(6):3398–3407. [PubMed: 16321982]
4. Xiao YJ, Schwartz B, Washington M, Kennedy A, Webster K, Belinson J, Xu Y. Anal Biochem 2001;290(2):302–313. [PubMed: 11237333]
5. Rother E, Brandl R, Baker DL, Goyal P, Gebhard H, Tigyi G, Siess W. Circulation 2003;108(6):741–747. [PubMed: 12885756]
6. Zhang C, Baker DL, Yasuda S, Makarova N, Balazs L, Johnson LR, Marathe GK, McIntyre TM, Xu Y, Prestwich GD, Byun HS, Bittman R, Tigyi G. J Exp Med 2004;199(6):763–774. [PubMed: 15007093]
7. Siess W, Zangl KJ, Essler M, Bauer M, Brandl R, Corrinth C, Bittman R, Tigyi G, Aepfelbacher M. Proc Natl Acad Sci U S A 1999;96(12):6931–6936. [PubMed: 10359816]
8. Rizza C, Leitinger N, Yue J, Fischer DJ, Wang DA, Shih PT, Lee H, Tigyi G, Berliner JA. Lab Invest 1999;79(10):1227–1235. [PubMed: 10532586]
9. Lin CI, Chen CN, Chen JH, Lee H. J Cell Biochem 2006;99(4):1216–1232. [PubMed: 16795034]
10. Tokumura A, Iimori M, Nishioka Y, Kitahara M, Sakashita M, Tanaka S. Am J Physiol 1994;267(1 Pt 1):C204–210. [PubMed: 8048480]
11. Hayashi K, Takahashi M, Nishida W, Yoshida K, Ohkawa Y, Kitabatake A, Aoki J, Arai H, Sobue K. Circ Res 2001;89(3):251–258. [PubMed: 11485975]
12. Angeli V, Llodra J, Rong JX, Satoh K, Ishii S, Shimizu T, Fisher EA, Randolph GJ. Immunity 2004;21(4):561–574. [PubMed: 15485633]
13. Llodra J, Angeli V, Liu J, Trogan E, Fisher EA, Randolph GJ. Proc Natl Acad Sci U S A 2004;101(32):11779–11784. [PubMed: 15280540]
14. Siess W. Pathophysiol Haemost Thromb 2006;35(3–4):292–304. [PubMed: 16877878]
15. Fueller M, Wang DA, Tigyi G, Siess W. Cell Signal 2003;15(4):367–375. [PubMed: 12618211]
16. Yoshida K, Nishida W, Hayashi K, Ohkawa Y, Ogawa A, Aoki J, Arai H, Sobue K. Circulation 2003;108(14):1746–1752. [PubMed: 14504178]
17. Diep QN, Schiffrin EL. Hypertension 2001;38(2):249–254. [PubMed: 11509485]
18. Li AC, Glass CK. Nat Med 2002;8(11):1235–1242. [PubMed: 12411950]

19. Leesnitzer LM, Parks DJ, Bledsoe RK, Cobb JE, Collins JL, Consler TG, Davis RG, Hull-Ryde EA, Lenhard JM, Patel L, Plunket KD, Shenk JL, Stimmel JB, Therapontos C, Willson TM, Blanchard SG. Biochemistry 2002;41(21):6640–6650. [PubMed: 12022867]
20. Lim S, Jin CJ, Kim M, Chung SS, Park HS, Lee IK, Lee CT, Cho YM, Lee HK, Park KS. Arterioscler Thromb Vasc Biol 2006;26(4):808–813. [PubMed: 16424348]
21. Lee CS, Kwon YW, Yang HM, Kim SH, Kim TY, Hur J, Park KW, Cho HJ, Kang HJ, Park YB, Kim HS. Arterioscler Thromb Vasc Biol 2009;29(4):472–479. [PubMed: 19201691]
22. Guo H, Makarova N, Cheng YES, Ji RR, Zhang C, Farrar P, Tigyi G. Biochim Biophys Acta 2008;1781(9):571–581. [PubMed: 18602022]
23. Contos JJ, Fukushima N, Weiner JA, Kaushal D, Chun J. Proc Natl Acad Sci U S A 2000;97(24): 13384–13389. [PubMed: 11087877]
24. Contos JJ, Ishii I, Fukushima N, Kingsbury MA, Ye X, Kawamura S, Brown JH, Chun J. Mol Cell Biol 2002;22(19):6921–6929. [PubMed: 12215548]
25. Yang AH, Ishii I, Chun J. Biochim Biophys Acta 2002;1582(1–3):197–203. [PubMed: 12069829]
26. Schneider A, Zhang Y, Guan Y, Davis LS, Breyer MD. Am J Physiol Renal Physiol 2003;284 (2):F411–417. [PubMed: 12529277]
27. Akiyama TE, Sakai S, Lambert G, Nicol CJ, Matsusue K, Pimprale S, Lee YH, Ricote M, Glass CK, Brewer HB Jr, Gonzalez FJ. Mol Cell Biol 2002;22(8):2607–2619. [PubMed: 11909955]
28. Jones JR, Shelton KD, Guan Y, Breyer MD, Magnuson MA. Genesis 2002;32(2):134–137. [PubMed: 11857800]
29. Guan Y, Hao C, Cha DR, Rao R, Lu W, Kohan DE, Magnuson MA, Redha R, Zhang Y, Breyer MD. Nat Med 2005;11(8):861–866. [PubMed: 16007095]
30. Jones JR, Barrick C, Kim KA, Lindner J, Blondeau B, Fujimoto Y, Shiota M, Kesterson RA, Kahn BB, Magnuson MA. Proc Natl Acad Sci U S A 2005;102(17):6207–6212. [PubMed: 15833818]
31. Fujiwara Y, Sardar V, Tokumura A, Baker D, Murakami-Murofushi K, Parrill A, Tigyi G. J Biol Chem 2005;280(41):35038–35050. [PubMed: 16115890]
32. Williams JR, Khandoga AL, Goyal P, Fells JI, Perygin DH, Siess W, Parrill AL, Tigyi G, Fujiwara Y. J Biol Chem. 2009
33. Bandoh K, Aoki J, Taira A, Tsujimoto M, Arai H, Inoue K. FEBS Lett 2000;478(1–2):159–165. [PubMed: 10922489]
34. Levy AP, Levy JE, Kalet-Litman S, Miller-Lotan R, Levy NS, Asaf R, Guetta J, Yang C, Purushothaman KR, Fuster V, Moreno PR. Arterioscler Thromb Vasc Biol 2007;27(1):134–140. [PubMed: 17068284]
35. Papaspyridonos M, McNeill E, de Bono JP, Smith A, Burnand KG, Channon KM, Greaves DR. Arterioscler Thromb Vasc Biol 2008;28(3):433–440. [PubMed: 18096829]
36. Seimon TA, Wang Y, Han S, Senokuchi T, Schrijvers DM, Kuriakose G, Tall AR, Tabas IA. J Clin Invest 2009;119(4):886–898. [PubMed: 19287091]
37. Kaneyuki U, Ueda S, Yamagishi S, Kato S, Fujimura T, Shibata R, Hayashida A, Yoshimura J, Kojiro M, Oshima K, Okuda S. Vascul Pharmacol 2007;46(4):286–292. [PubMed: 17178255]
38. Lin DA, Boyce JA. J Immunol 2005;175(8):5430–5438. [PubMed: 16210650]
39. Yokoyama K, Baker DL, Virag T, Liliom K, Byun H, Tigyi G, Bittman R. Biochim Biophys Acta 2002;1582:295–308. [PubMed: 12069841]
40. Fischer DJ, Nusser N, Virag T, Yokoyama K, Wang D, Baker DL, Bautista D, Parrill AL, Tigyi G. Mol Pharmacol 2001;60(4):776–784. [PubMed: 11562440]
41. Sano T, Baker D, Virag T, Wada A, Yatomi Y, Kobayashi T, Igarashi Y, Tigyi G. J Biol Chem 2002;277(24):21197–21206. [PubMed: 11929870]
42. Lin CI, Chen CN, Lin PW, Chang KJ, Hsieh FJ, Lee H. Biochem Biophys Res Commun 2007;363 (4):1001–1008. [PubMed: 17923111]

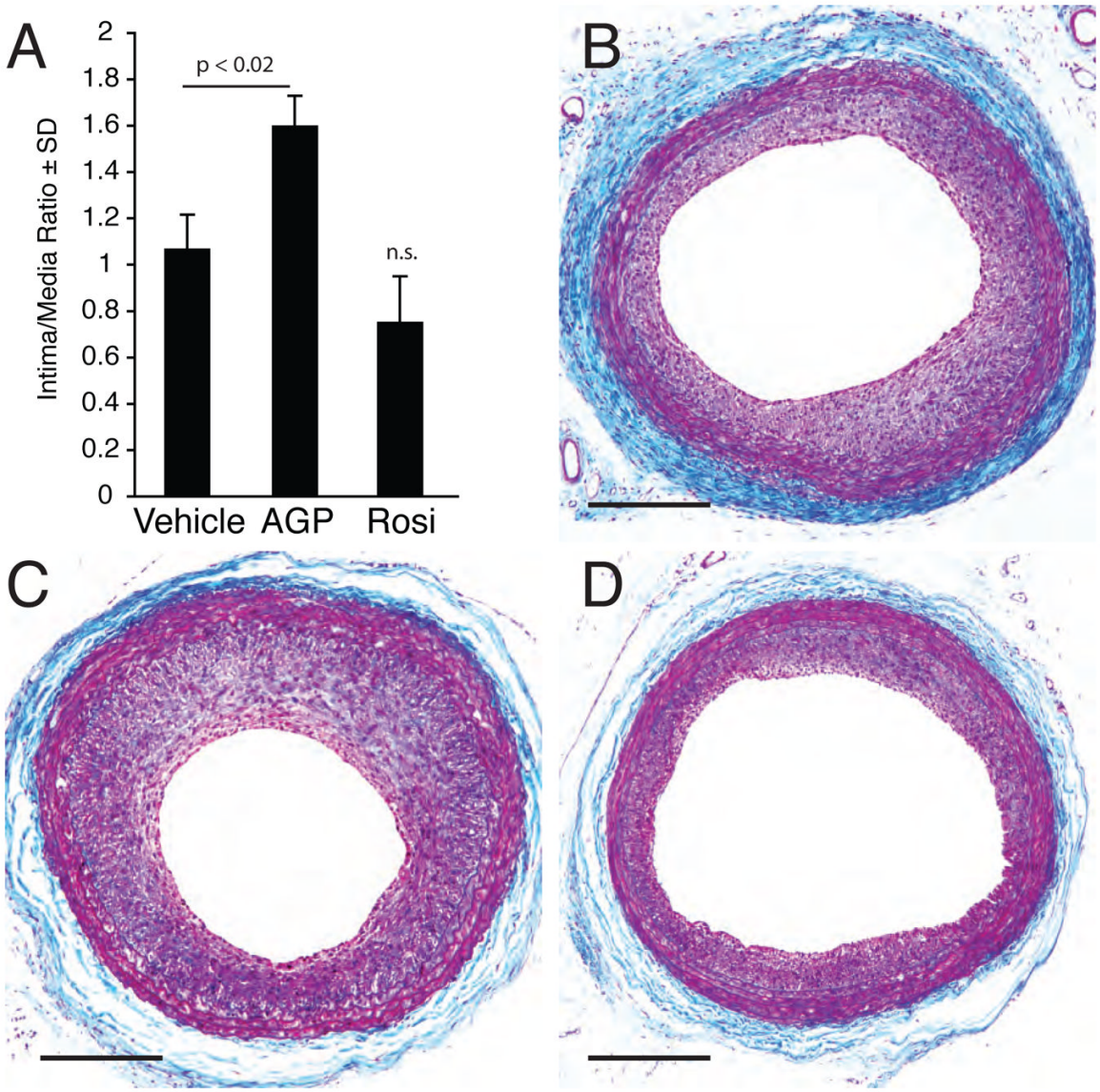

Figure 1.

Effects of 10 μM AGP or ROSI on neointima induced by balloon injury of the rat carotid artery. Panel A: Intima-to-media ratios three weeks after balloon injury followed by a one-hour treatment with vehicle, 10 μM AGP or ROSI. Panels B, C, and D show representative cross sections of vehicle-, AGP-, and ROSI-treated carotid arteries. The calibration bar is 200 μm.

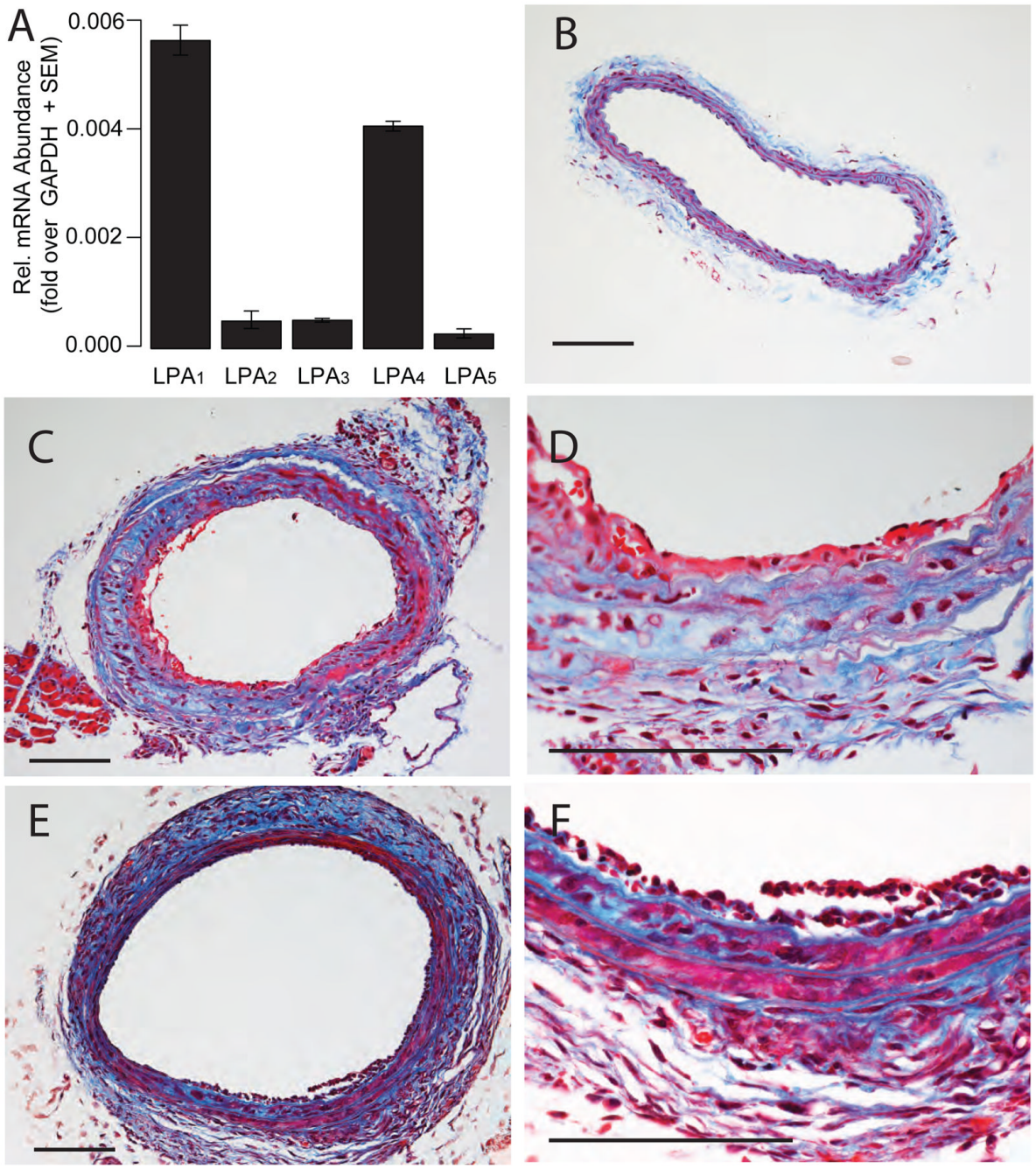

Figure 2.

AGP and ROSI elicit arterial wall remodeling in C57/BL6 mouse carotids. Panel A: Quantitative RT-PCR of LPA GPCR expression in the mouse carotid artery. Panel B: Trichrome-stained cross section of a C57/BL6 mouse carotid treated with vehicle. Panels C & D: Cross section of a trichrome stained mouse common carotid artery three weeks after intralumenal application of 2.5 μM AGP. Panel C: Cross section of a mouse common carotid artery three weeks after intralumenal application of 2.5 μM ROSI. Trichrome staining, the bars are 100 μm. Note the multi-layered neointima and changes in the media indicated by the blue stain.

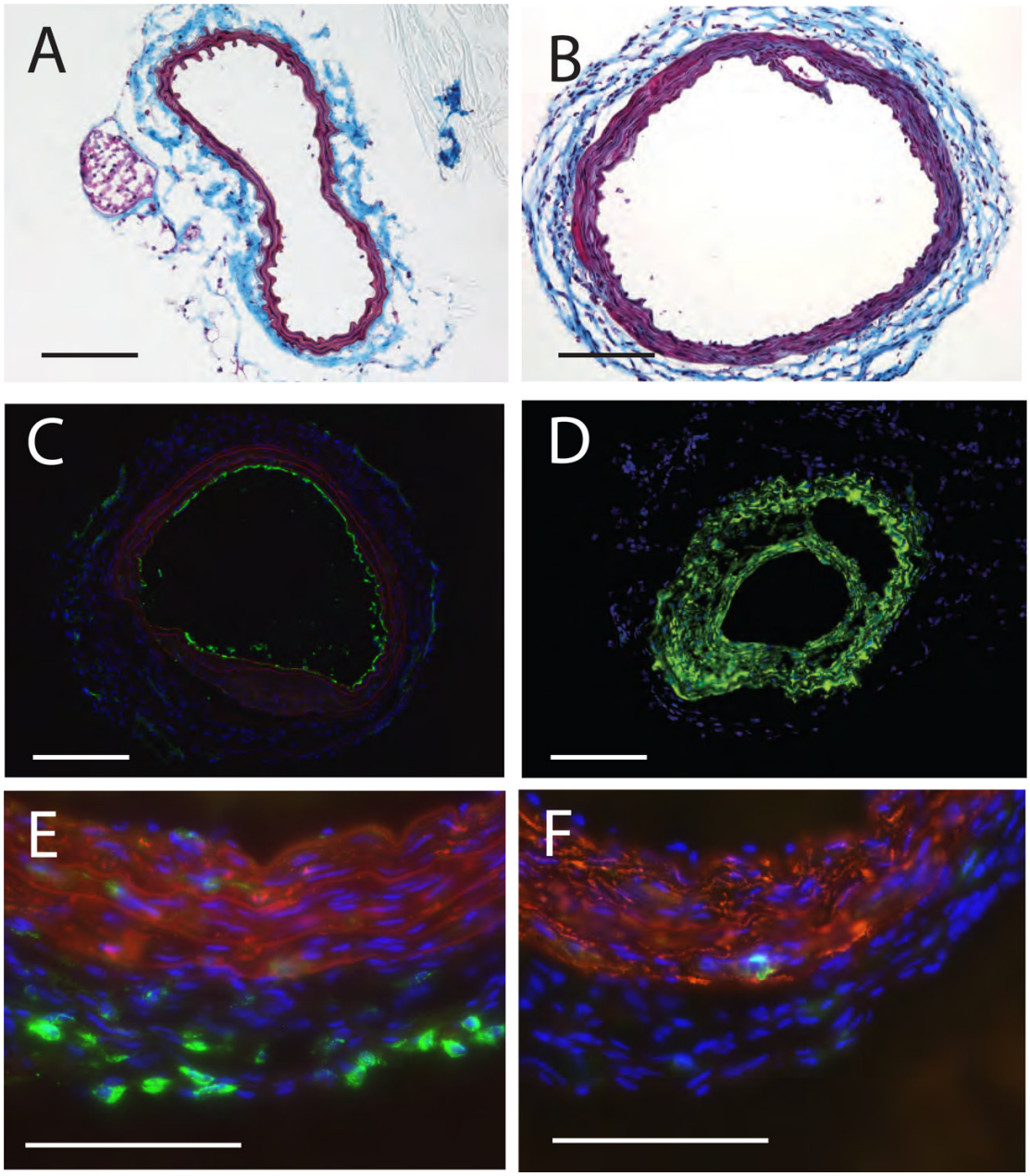

Figure 3.

Histological and immunohistological staining of neointima in C57/BL6 mouse carotids three weeks after intralumenal application of 2.5 μM AGP. Panel A. Vehicle injected control carotid artery shows no neointima. Panel B: AGP-treatment causes concentric neointima with capillary formation within the neointima. Panel C: Anti-CD31 staining shows single layer of staining and lack of staining in the neointimal layers. Panel D. Anti-αSMA staining shows intensive immunoreactivity in the neointimal layers. Panel E. Merged image of anti-CD68 (green) and anti-αSMA (red) staining shows scattered cells bearing this marker in the neointima and no double stained cells in this merged image. Panel F. Anti-CD11b stained cells are few and anti-αSMA double positive cells are not visible. Calibration bar is 100 μm.

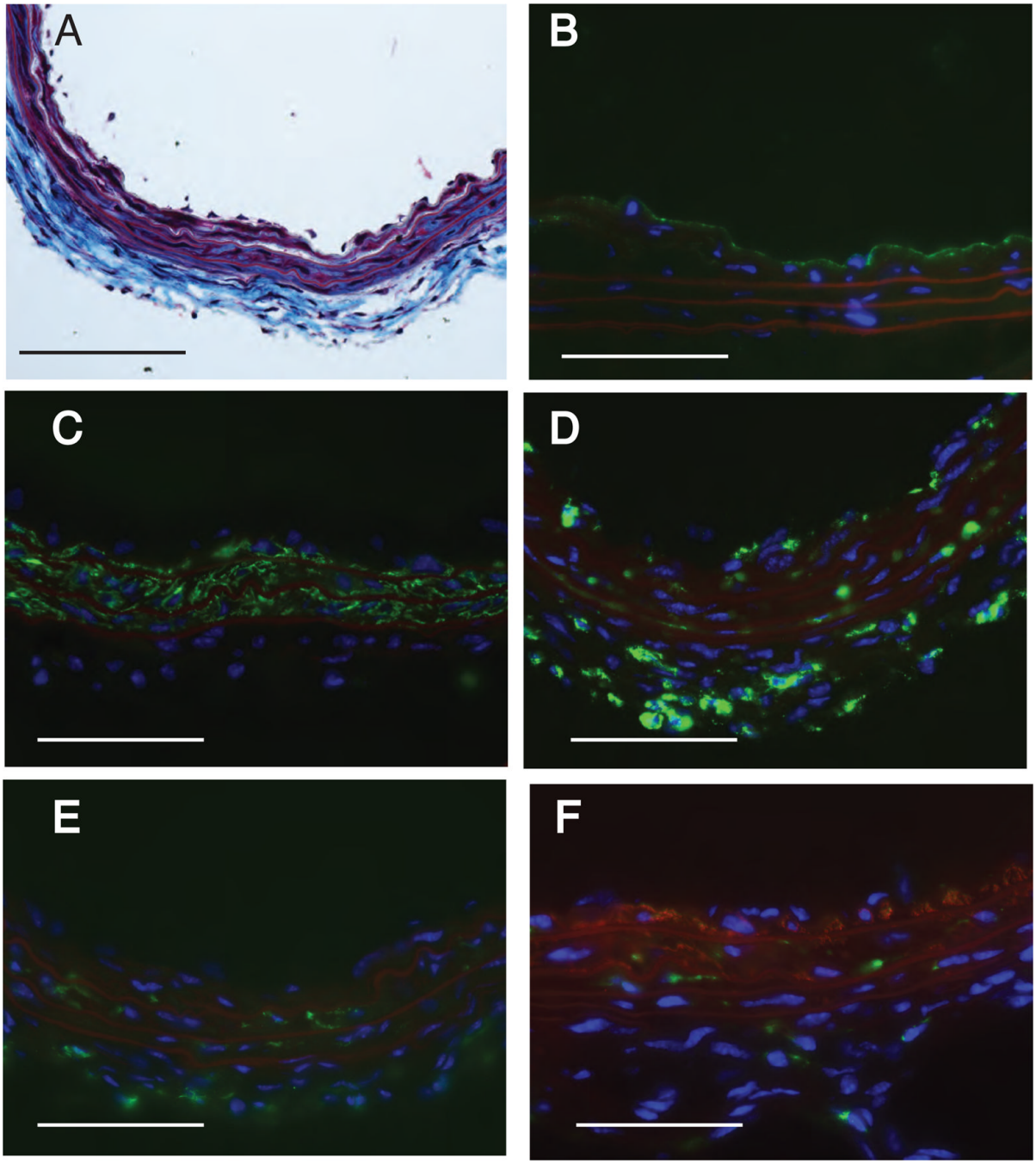

Figure 4.

Histological and immunohistological staining of neointima three weeks after intralumenal application of 2.5 μM ROSI into the carotid of WT C57BL/6 mice. Panel A. Masson's trichrome stain shows multi-layered neointima. Panel B: Anti-CD31 staining shows lack of staining in the neointimal layers. Panel C. Anti-αSMA staining shows intensive positivity of the neointimal layers. Panel D. Anti-CD68 stains cells bearing this marker in the neointima and at the media-adventitia boundary. Panel E. No anti-CD11b stained cells are detected in the neointima. Panel F. Merged image of double staining with anti-CD11b (green) and anti-αSMA (red) shows distinct populations of cells bearing only one but not both markers. Calibration bar is 100 μm.

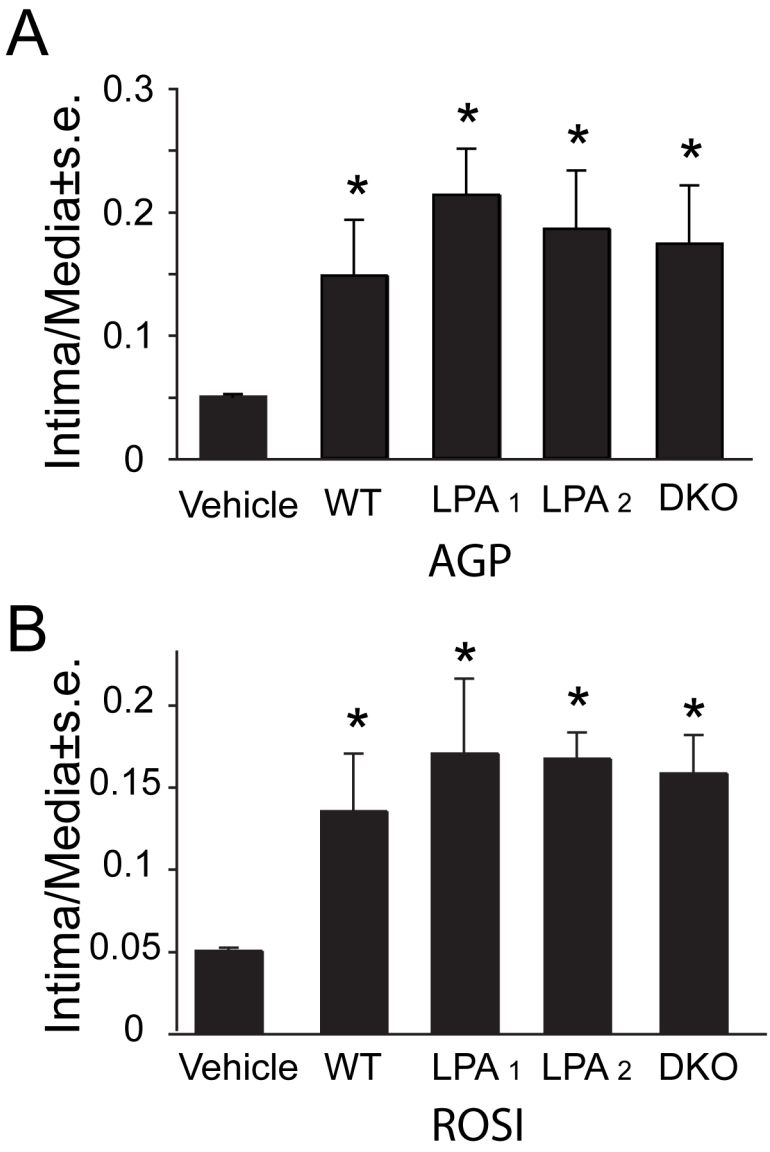

Figure 5.

Intima-to-media ratios measured in WT and LPA_1, LPA_2, and DKO mice. Effect of 2.5 μM intralumenal application of either AGP (panel A) or ROSI (panel B) three weeks after treatment. Note the similar intima-to-media ratios elicited by the treatments regardless of the genotype of the mice. No statistically significant differences were found between the different KOs.

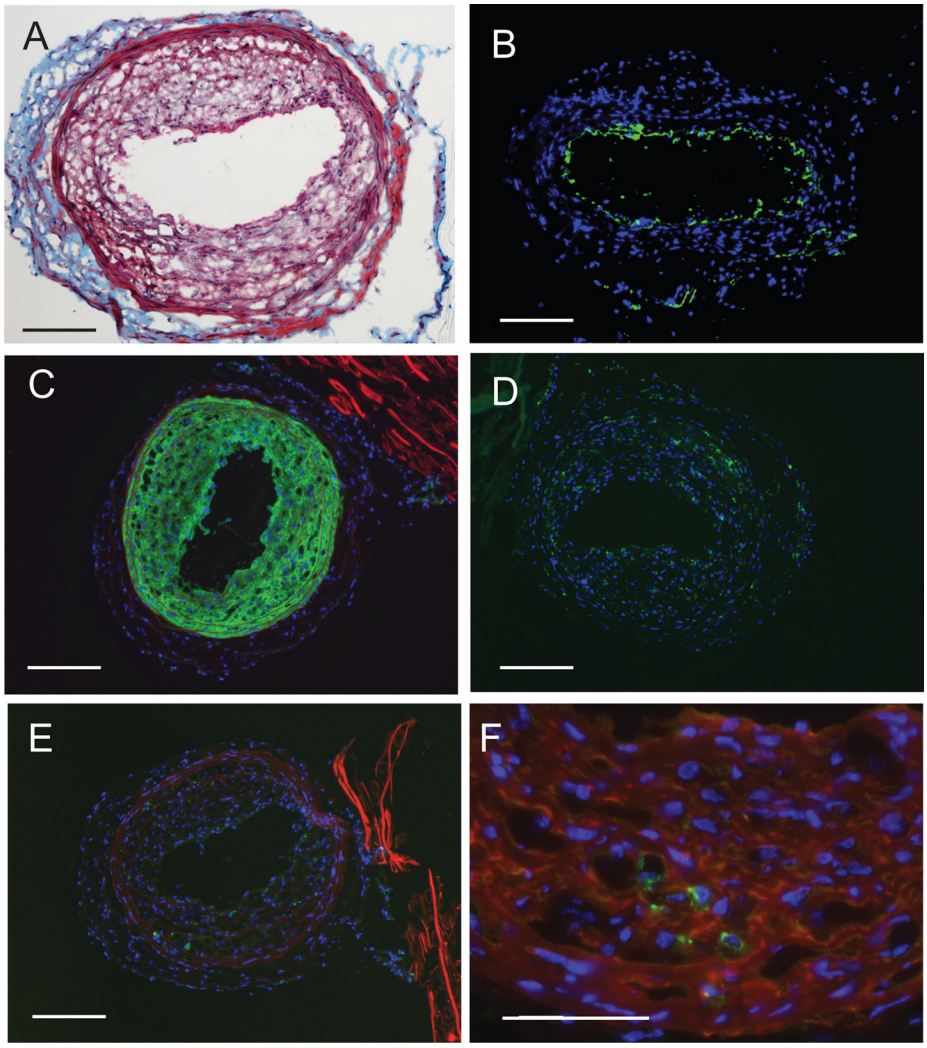

Figure 6.

Immunohistological phenotyping of neointima three weeks after intralumenal application of 5 μM AGP in DKO mice. Panel A: Masson trichrome-stained carotid shows multi-layered neointima. Panel B: Anti-CD31 staining shows lack of staining in the neointimal layers. Panel C. Anti-αSMA staining shows intensive immunoreactivity in the neointimal layers. Panel D. Anti-CD68 staining shows positive cells in the neointima. Panel E. Anti-CD11b stained cells are few and localized at the media-to-adventitia border. Panel F: Merged double staining for CD11n (green) and anti-αSMA staining shows no double positive cell. Calibration bar is 100 μm.

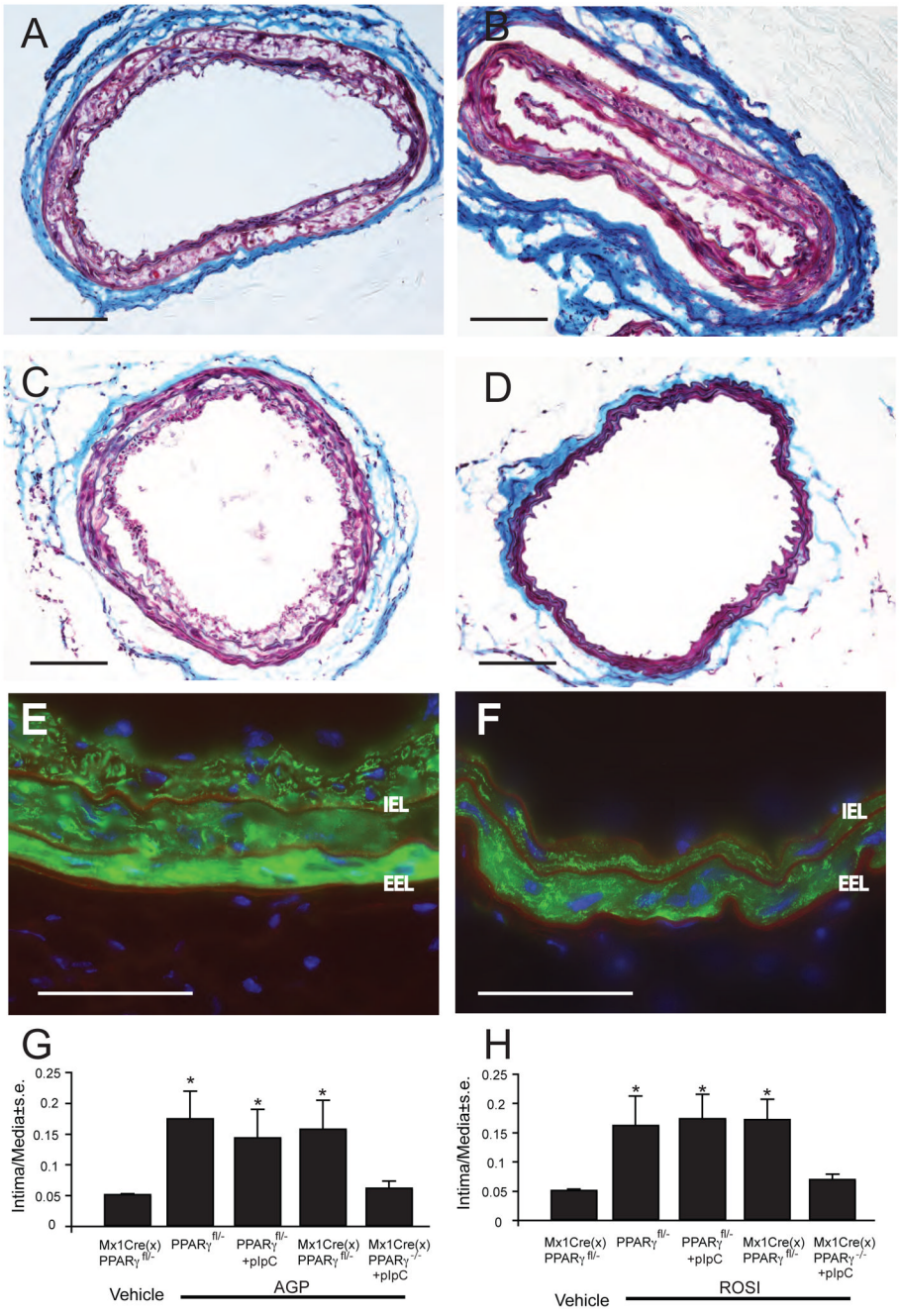

Figure 7.

Effect of Mx1Cre-mediated conditional knock out of PPARγ on AGP-induced neointima. Panel A: Trichrome staining of a representative Mx1Cre transgenic mouse carotid three weeks after exposure to 2.5 μM AGP. Panel B: Representative trichrome-stained carotid of a pIpC-induced PPARγ$^{fl/-}$ mouse three weeks after AGP treatment. Panel C: Trichrome-stained mouse carotid from a Mx1CreXPPARγ$^{fl/-}$ mouse without pIpC induction three weeks after exposure to 2.5 μM AGP. Panel D: Trichrome-stained carotid from a pIpC-induced ΔPPARγ mouse three weeks after AGP treatment. Note the complete lack of neointima development. Panel E: Anti-αSMA staining of an uninduced Mx1CreXPPARγ$^{fl/-}$ mouse three weeks after AGP treatment. Note the αSMA positive neointimal cells inside the internal elastic lamina (IEL) that

shows red autofluorescence. EEL- external elastic lamina. Panel F: Anti-αSMA staining of an pIpC-induced ΔPPARγ mouse three weeks after AGP treatment. Note the complete lack of αSMA staining inside the IEL. Calibartion bars are 100 μm. Intima to media ratios in mice with or without pIpC induction three weeks after exposure to 2.5 μm AGP (panel G) or ROSI (panel H). Asterisks denote significant differences to uninduced vehicle-treated Mx1CreXPPARγ$^{fl/-}$ mice ($p < 0.05$, n= 5–10 mouse per group).

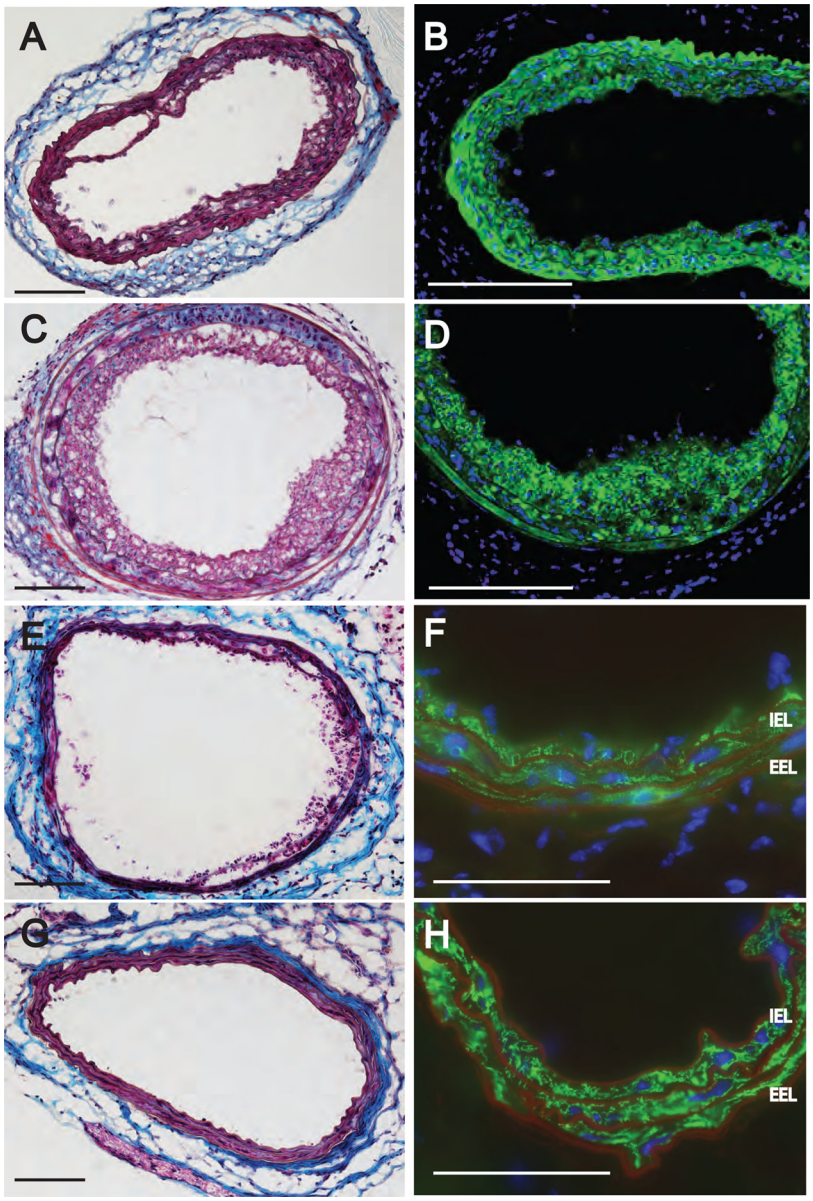

Figure 8.

Effect of Mx1Cre-mediated conditional knock out of PPARγ on ROSI-induced neointima. Trichrome (panel A) and anti-αSMA (panel B) staining of a pIpC-treated Mx1Cre mouse carotid three weeks after treatment with 2.5 μM ROSI. Trichorme (panel C) and anti-αSMA (panel D) staining of a carotid from a pIpC-induced $PPAR\gamma^{fl/-}$ mouse. Trichorme (panel E) and anti-αSMA (panel F) staining of a carotid from a non-pIpC-induced $Mx1CreXPPAR\gamma^{fl/-}$ mouse carotid. Note the anti-αSMA positive neointimal cells inside the IEL. Trichorme (panel G) and anti-αSMA (panel H) staining of an pIpC-induced ΔPPARγ mouse three weeks after ROSI treatment. Note the complete lack of αSMA staining inside the IEL. Calibartion bars are 100 μm.